

Co(II), Ni(II), Pd(II), Pt(IV), Cu(II) and UO₂(II)-Ethanethiohydrazide Derivative Complexes: Synthesis, Spectral, Thermal and Computational Study

KHLOOD SAAD ABOU-MELHA

Chemistry Department, Faculty of Science, King Khalid University, P.O. Box 9004, Abha, Saudi Arabia

Corresponding author: Tel: +966 555761800; E-mail: dr.khlood@hotmail.com

Received: 27 April 2015;

Accepted: 3 June 2015;

Published online: 29 August 2015;

AJC-17520

A new series of metal ion complexes were synthesized using a SNSN donor ligand. The prepared complexes were characterized by FTIR, ESR, XRD, TG/DTA and SEM. The IR and ¹H NMR spectra of the ligand show the presence of its tautomeric forms (thione-thiol). The ligand forms were contributed at Pd(II), Co(II), Ni(II) and Cu(II) complexes as a neutral tetradentate coordinator towards two central nucleus. While, in case of Pt(IV) and UO₂(II) complexes, the ligand contributes as bi-negative tetradentate. The proposed geometries are in-between six to four coordination number surround the central atoms. The geometries proposed refer to the electronic spectral data beside the magnetic measurements. The XRD patterns reflect the nano-crystalline structures for the ligand, Pd(II), UO₂(II) and Ni(II) compounds but the others are in amorphous in nature. The SEM images show undefined shapes except the needles ligand and granules Cu(II) complex shapes. EPR spectrum of Cu(II) complex is verifying the square-planar geometry of the complex through the calculating the spin Hamiltonian parameters. The TG and DTG curves displaying the lower thermal stability as a general trend. The molecular modeling was performed to assign the structural formula proposed for the ligand and its relative complexes.

Keywords: Thiohydrazide complexes, X-ray diffractions, Molecular modeling, EPR spectra.

INTRODUCTION

Compounds containing thione (C=S) and thiol (C-S) groups occupy an important position among organic reagents as potential donor ligands for transition metal ions¹. Both the organic compounds and their metal complexes display a wide range of pharmacological activity including anticancer antibacterial and fungi static effects. Coordination chemistry of SN donors has been a subject of enthusiastic research since they show a wide range of biological properties. Also, SN donor ligands are versatile ligands having *p*-delocalization of charge and configurational flexibility of the molecular chain that can rise the coordination modes owing to the interest. They generate variety of biological properties ranging from anticancer, antitumor, antifungal antibacterial, antimalarial, antifilarial, antiviral and anti-HIV activities¹⁻⁵. They can also yield mono or polynuclear complexes some of which are biologically relevant⁶. Here in present study, the author focuses on preparing a simple ligand by includes SNNS donors distributed by away permeate the presence of bi-nucleus centers which may serve distinguish in biological field. A thiohydrazide ligand was prepared from *p*-chlorophenylisothiocyanate compound. A series of Pt(IV), Pd(II), UO₂(II), Ni(II), Cu(II) and Co(II) complexes were prepared. The chemistry of all

complexes will be investigated to emphasis on their molecular and structural formula. The molecular modeling will also use to assert on the orientation of active sites in the organic compound and also investigating the isolated complexes. Also, the biological behaviour of the organic ligand was theoretically predicted towards different biotechnical processes.

THEORETICAL METHODOLOGIES

Molecular modeling: A trial to obtain an acceptable insight about the best orientation of SNNS active sites in molecular modeling of the ligand (Fig. 1). The geometry optimization and conformational analysis has been performed by the use of MM+⁷ force-field as implemented in Hyperchem 5.1⁸ to draw the most stable geometries.

Drug-likeness calculations: Molinspiration strategy is used to calculate the drug-likeness score, also focus on particular drug classes and development of specific activity score for each of these classes. The method we implemented uses sophisticated Bayesian statistics to compare structures of representative ligands active on the particular target with structures of inactive molecules and to identify substructure features (which in turn determine physicochemical properties) typical for active molecules.

EXPERIMENTAL

Carbon, hydrogen and nitrogen were analyzed using a Perkin-Elmer CHN 2400 in the Micro-analytical Unit at the Faculty of Science, Cairo University, Egypt. The metal content was determined using complexometric titrations and the Cl content was tested gravimetrically using AgNO_3 . The molar conductivities of freshly prepared $1.0 \times 10^{-3} \text{ mol/cm}^3$ DMSO solutions were measured using Jenway 4010 conductivity meter. The infrared spectra, as KBr discs, were recorded on a Mattson 5000 FTIR spectrometer ($4000\text{-}400 \text{ cm}^{-1}$), Mansoura University. The proton NMR spectra were recorded on a Varian FT-500 MHz spectrometer in $\text{DMSO-}d_6$ as a solvent and TMS as internal standard, King Khalid University. The electronic spectra were recorded in DMSO solvent, in range 200-900 nm using Unicam UV/vis spectrometer, Mansoura University. The effective magnetic moments were evaluated at room temperature by applying $\mu_{\text{eff}} = 2.84 \sqrt{X_M T}$, where X_M is the molar susceptibility corrected using Pascal's constants for the diamagnetism of all atoms in the ligand using a Johnson Matthey magnetic susceptibility balance. The ESR spectrum of solid Cu(II) complex was obtained on a Bruker EMX Spectrometer working in the X-band (9.78 GHz) with 100 kHz modulation frequency. The microwave power was set at 1 mW and modulation amplitude was set at 4 Gauss. The low field signal was obtained after 4 scans with a 10 fold increase in the receiver gain. A spectrum was obtained in a 2 mm quartz capillary at room temperature. Differential thermal analysis (DTA) and thermogravimetric analysis (TGA) experiments were conducted using Shimadzu DTA-50 and Shimadzu TGA-50H thermal analyzers, respectively at Micro Analytical Center, King Khalid University. All experiments were performed using a single loose top loading platinum sample pan under nitrogen atmosphere at a flow rate of 30 mL/min and a 10°C/min heating rate for the temperature range 25-800 $^\circ\text{C}$. X-ray diffraction patterns of the samples were recorded on a X Pert Philips X-ray diffractometer. All the patterns were obtained by using $\text{CuK}\alpha_1$ radiation, with a graphite monochromator at $0.02^\circ/\text{min}$ scanning rate. The metal complexes were made in the form of tablets, which have $\approx 0.1 \text{ cm}$ thickness, under a pressure of approximately $5 \times 10^7 \text{ Pa}$. Scanning electron microscopy images were taken in Joel JSM-6390 equipment.

4-Chlorophenylisothiocyanate and hydrazine hydrate compounds were of analytically reagent grade, commercially available from Fulka and used without previous purification. Also, $\text{UO}_2(\text{NO}_3)_2 \cdot 6\text{H}_2\text{O}$, $\text{CoCl}_2 \cdot 6\text{H}_2\text{O}$, $\text{Ni}(\text{NO}_3)_2 \cdot 6\text{H}_2\text{O}$, $\text{CuCl}_2 \cdot 2\text{H}_2\text{O}$, PtCl_2 , PdCl_2 and PtCl_4 were purchased from Merck Co.

Synthesis of H_2L ligand: 4-Chlorophenylisothiocyanate (10 mmol, 1.696 g) was dissolved into 50 mL ethanol, 20 mL of hydrazine hydrate (5 mol) was added drop-wise then worm for 20 min heating again for further 40 min, allow to cool down. Collect the product by filtration, wash with ethanol, ether and recrystallized in ethanol. The isolated 2-(4-chlorophenyl)- N' -(2-(4-chlorophenyl)ethanethiyl)ethanethio-hydrazide ($\text{C}_{16}\text{H}_{14}\text{N}_2\text{S}_2\text{Cl}$) (Fig. 1A and 1B) by 76 % yield and the elemental analysis of: C 52.01, H 3.80, N 7.45. The ^1H NMR spectrum ($\text{DMSO-}d_6$, 500 MHz) given in Fig. 2A showed; δ

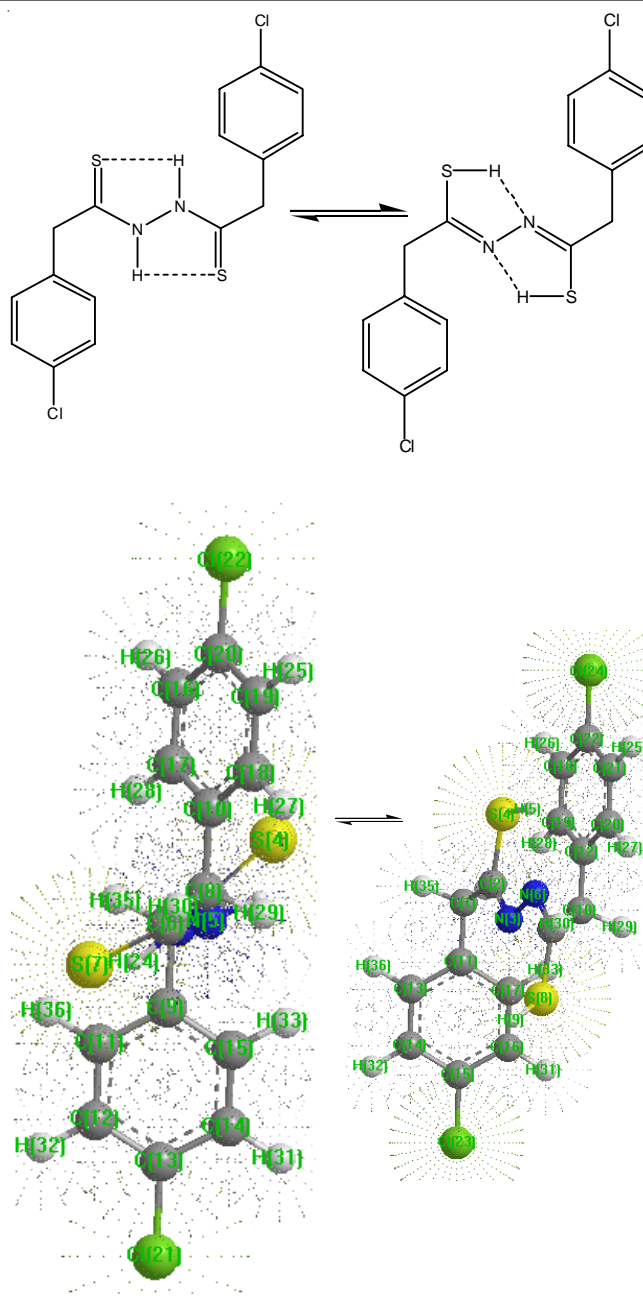


Fig. 1. Structural form of 2-(4-chlorophenyl)- N' -(2-(4-chlorophenyl)ethanethiyl)ethanethiohydrazide ($\text{C}_{16}\text{H}_{14}\text{N}_2\text{S}_2\text{Cl}$) H_2L ligand and its molecular thionio (A)-thiol (B) modeling forms

ppm = 1.2 (s, SH), 2.51 (s, 2NH or CH_2), 3.34 (s, H_2O in DMSO), 7.33-7.72 (m, Ph-Cl). The presence of a peak assigned to SH proton ($\delta = 1\text{-}1.5 \text{ ppm}$) supports the presence of thionio-thiol tautomeric forms. ^{13}C NMR (ppm) showed the peaks at; 179.34 (C=S) or (C=N) groups and at 40.11 for CH_2 , 125.2-138.3 (Ph carbons) and 38.86-40.02 (DMSO). The calculated distribution of activity scores for the ligand forms (version 2011.06) towards GPCR ligands, kinase inhibitors, ion channel modulators, nuclear receptor ligands, protease inhibitors and other enzyme targets compared with scores for about 100'000 average drug-like molecules were done. The score allows efficient separation of active and inactive molecules. The results show: GPCR (G protein-coupled receptor) ligand -0.09 and 0.23, ion channel modulator -0.14 and 0.29, Kinase inhibitor

-0.23 and -0.01, Nuclear receptor ligand-0.18 and 0.07, Protease inhibitor -0.25 and -0.04 and Enzyme inhibitor -0.12 and 0.07, for thion-thiol forms, respectively. The data display the nearer results in-between the investigated thion form and the known drugs especially with GPCR and Enzyme inhibitor. The thiol form display a great difference in-between the behaviour of the compound and the compared drugs in all calculated bioactive process.

Synthesis of metal complexes: The M-H₂L complexes were prepared by refluxing H₂L (0.735 g, 2 mmol) with 2 mmol of each metal salt; 0.476 g of CoCl₂·6H₂O, 0.582 g of Ni(NO₃)₂·6H₂O, 0.341 g of CuCl₂·2H₂O, 0.355 g of PdCl₂, 0.674 g of PtCl₄ and 1.004 g UO₂(NO₃)₂·6H₂O in 20 mL ethanol for 3 h. A little amount of solid KCl was added with Pt(IV) and Pd(II) salts solutions for complete dissolution. The Pt(IV) complex was isolated after the addition of about 0.5 g sodium acetate and also, uranyl complex was isolated after the addition of few drops of diluted NaOH solution. The resulting metal complexes were filtered off while hot, washed with ethanol followed by diethyl ether and dried in vacuum over CaCl₂. ¹H NMR spectrum of Pt(IV) complex (DMSO-*d*₆, 500MHz) given in Fig. 2B shows; δ ppm = 7.24-7.46 (m, 8H, 2Ph-Cl), intense peak at 4.02 (s, H₂O in DMSO and complex), 2.513 (s, 4H, CH₂), 2.52 (s, CH₃ of OAc) and 2.51 (s, DMSO). While the ¹³C NMR showed the bands at 149.55 (C=N), 128.31-128.91 (2Ph-Cl), (2Ph-Cl) and 40.01 (2CH₂) and 39.93-39.00 (DMSO). The ¹H NMR of Pd(II) complex (DMSO-*d*₆, 500 MHz) given in Fig. 2C show the peaks at δ ppm = 7.43-8.51 (m, 8H, 2Ph-Cl), a broad peak centered at 3.84 (s, H₂O in complex and NH groups), 2.513 (s, 4H, CH₂) and 2.51 (s, DMSO). While the ¹³C NMR showed the bands at 129.55 (C=S), 129.25-124.73 (2Ph-Cl), (2Ph-Cl) and 40.08 (2CH₂) and 38.83-39.99 (DMSO). The ¹H NMR of UO₂(II) complex (DMSO-*d*₆, 500MHz) given in Fig. 2D show the peaks at δ ppm = 7.04-7.44 (m, 8H, 2Ph-Cl), at 3.35 (s, H₂O in complex and DMSO), 2.512 (s, 4H, CH₂) and 2.51 (s, DMSO). While the ¹³C NMR showed the bands at 149.55 (C=N), 129.25-124.73 (2Ph-Cl), (2Ph-Cl) and 40.08 (2CH₂) and 38.83-39.99 (DMSO).

RESULTS AND DISCUSSION

All the physical properties and analytical results of the prepared compounds were summarized in Table-1. The elemental analysis proposed the presence of 1:2 (L:M) molar ratio isolated for all investigated complexes which is expected during draw the base line of present study.

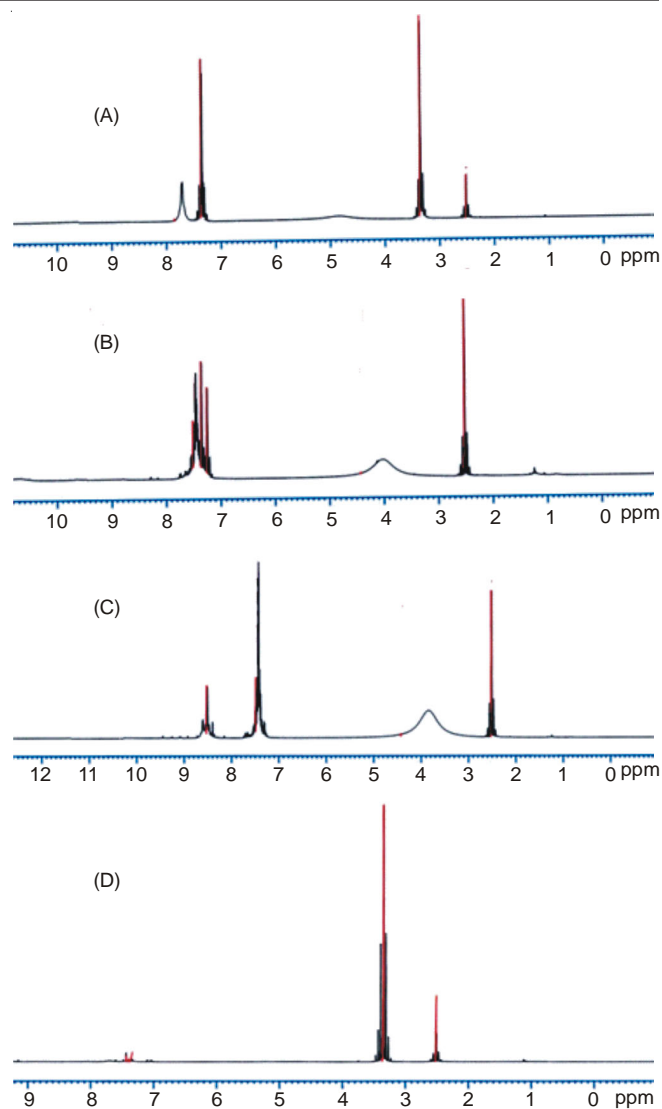


Fig. 2. ¹H NMR spectra of the free ligand, Pd(II), Pt(IV) and UO₂(II) complexes, (A, B, C and D, respectively)

Molar conductance: The conductivity measurements were performed for clear solution in DMSO as a solvent at room temperature. The molar conductivity values for 10⁻³ mol/cm³ of three soluble complexes (Co, Cu and Pd(II) complexes) were found to be 14-20 ohm⁻¹ cm² mol⁻¹, respectively, suggesting the non-electrolytic nature of these complexes^{10,11}. It was observed that, the relatively acidic medium favour the occlusion of the conjugated anions inside the coordination.

IR, ¹H NMR and ¹³C NMR spectra: The infrared absorption spectra are considered the best qualitative tool used for

TABLE-1
ANALYTICAL DATA FOR LIGAND (H₂L) AND ITS METAL COMPLEXES

Compound	Color	Elemental analysis (%): Calcd. (Found)					Λ (Ω ⁻¹ cm ² mol ⁻¹)
		C	H	N	M	Cl	
C ₁₆ H ₁₄ N ₂ S ₂ Cl ₂ (H ₂ L)	Creamy	52.03 (52.01)	3.82 (3.80)	7.58 (7.45)	–	19.19 (19.20)	5.4
[Pt ₂ (OAc) ₆ (C ₁₆ H ₁₂ N ₂ S ₂ Cl ₂)·2H ₂ O]H ₂ O	Dark green	28.85 (28.84)	3.11 (3.10)	2.4 (2.3)	33.47 (33.45)	–	5.2
[Pd ₂ Cl ₄ (C ₁₆ H ₁₄ N ₂ S ₂ Cl ₂)]H ₂ O	Faint yellow	25.89 (25.54)	2.17 (2.16)	3.77 (3.79)	28.68 (28.70)	28.67 (28.71)	–
[(UO ₂) ₂ (NO ₃) ₂ (C ₁₆ H ₁₂ N ₂ S ₂ Cl ₂)·2H ₂ O]H ₂ O	Yellow	17.71 (17.72)	1.67 (1.66)	5.16 (5.12)	43.86 (43.87)	–	–
[Ni ₂ (NO ₃) ₄ (C ₁₆ H ₁₄ N ₂ S ₂ Cl ₂)·2H ₂ O]	Dark green	24.93 (24.95)	2.35 (2.33)	10.90 (10.88)	15.23 (15.24)	–	5.6
[Cu ₂ Cl ₄ (C ₁₆ H ₁₄ N ₂ S ₂ Cl ₂)]H ₂ O	Faint brown	28.50 (28.52)	2.69 (2.68)	4.15 (4.14)	18.85 (18.87)	31.55 (31.56)	6.1
[Co ₂ Cl ₄ (C ₁₆ H ₁₄ N ₂ S ₂ Cl ₂)]H ₂ O	Dark blue	28.89 (28.88)	2.73 (2.72)	4.21 (4.22)	17.72 (17.72)	31.98 (31.96)	5.4

proposing the mode of coordination in-between the organic ligand and the metal atoms. The spectrum of H₂L displays significant bands for two tautomeric forms (thion and thiol)¹². The band centered at 2400 cm⁻¹ assigned for ν(SH) band of thiol ligand. The following data supports the presence of the two forms; bands at 3292, 1587, 1535, 759, 648 and 1031 are assigned for ν(NH), δ(NH), ν(C=N), ν(C=S), νC-S and ν(N-N) respectively. Broadness around 1761 cm⁻¹ is proposing the intra ligand H-bonding in-between the neighboring active sites. These data are in agreement with ¹H NMR and ¹³C NMR results. All significant bands were summarized in Table-2 from a comparative study in-between the free ligand and its metal complexes. All metal complexes spectra display a broad band centered at 3440-3100 cm⁻¹ region, which could be attributed to ν(OH) of water molecules¹³. This introduced the presence of lattice and/or coordinated water in these complexes. The crystal water appears at frequencies higher than that of the coordination. The major vibration modes observed in the range 3430-3440 cm⁻¹ is a clear evidence for the presence of lattice water in all complexes. These non-ligand bands can be interpreted in term of presence of lattice and coordinated water molecules. This is supported through the thermogravimetric decomposition behaviour. There is no definite borderline between lattice and coordinated water molecules, especially in the stretching of OH and bending δ(H₂O) vibrations. Moreover, in the spectra of [Pd₂Cl₄(C₁₆H₁₄N₂S₂Cl₂)]H₂O, [Cu₂Cl₄(C₁₆H₁₄N₂S₂Cl₂)]2H₂O, [Co₂Cl₄(C₁₆H₁₄N₂S₂Cl₂)]2H₂O and [Ni₂(NO₃)₄(C₁₆H₁₄N₂S₂Cl₂)]2H₂O complexes, the ligand behaves as neutral tetradentate mode through S₂N₂ donors towards two metal atoms. This proposal is based on the following appearance; the lower shifted appearance of ν(C=S) bands especially IV one at about 730 cm⁻¹, the lower shifted appearance of ν(NH) and δ(NH) bands supports the participation of NH groups^{14,15}. This finding displays the coordination of thione tautomer form which may refer to the measurable stability of thione form in comparing with thiol one (will be discussed in modeling part). This behaviour is acceptable in relatively acidic medium produced by chloride or nitrate salts. The Ni(II) complex spectrum displays two bands at 1525 and 1456 cm⁻¹ assigned to ν_{asym} and ν_{sym}(NO₃) contributes as mono dentate anions inside the coordination¹⁶. In the [Pt₂(OAc)₆(C₁₆H₁₂N₂S₂Cl₂)·2H₂O]H₂O and [(UO₂)₂(NO₃)₂(C₁₆H₁₂N₂S₂Cl₂)·2H₂O]H₂O complexes spectra,

a complete obscure for ν(C=S) bands followed by the coherent appearance of ν(C=N) and ν(C-S) bands. This observation is proposing the coordination of ionized thiol form. This is acceptable with the addition of the sodium acetate during the precipitation of Pt(IV) complex as well as few drops of diluted NaOH during the precipitation of UO₂(II) complex. The two complexes spectra are displaying two bands assigned for the contribution of conjugated anions (OAc and NO₃, respectively) as a monodentate. Finally, new bands appeared at lower frequency region assigned to ν(M-N) and ν(M-S) vibrations were determined. The uranyl complex exhibits a significant band at 976 cm⁻¹ assigned to ν₃ vibration in-between four bands for dioxouranium ion¹⁷. The force constant (F) for the bonding sites of ν(U=O) is calculated by the method of McGlynn *et al.*¹⁸. (ν₃)² = (1307)²(F_{U-O})/14.1 The F_{U-O} value is 7.86 m dynes Å⁻¹, the U-O bond distance is calculated with the help of the equation shown as: R_{U-O} = 1.08 F^{1/3} + 1.17. The U-O bond distance (1.713 Å) falls in the usual region as reported earlier.

The mode of bonding in Pt(IV), UO₂(II) and Pd(II) complexes are verified from ¹³C NMR spectra through the lower appearance of C=N or C=S peaks in comparing with the original free ligand. Although, the ¹H NMR spectra are not introducing a strong evidence verifying the coordination mode due to the combined appearance of NH groups and crystal waters in the same position.

Electronic spectra and magnetic moments: The electronic spectral analysis was performed in DMSO covering the range 200–900 nm to assign the geometrical structure of the prepared metal complexes (Fig. 3). The results (Table-3) showed that the *d-d* splitting is strongly affected with the geometry surrounding the central atom. The absorption spectra recorded for most complexes emphasis on the absence of solvent interaction during the investigation. The Nujol mull was used to verify this proposal. Firstly, the H₂L ligand spectrum shows shoulders and bands in the range around 31,847; 26,738 and 23,474 cm⁻¹. The strong absorption bands at 31,847 and 26,738 cm⁻¹ can be assigned to π→π* transition and a medium absorption band at 23,474 cm⁻¹ may be assigned to charge transfer transition for n→π*[LMCT]¹⁹. The spectrum of [Pt₂(OAc)₆(C₁₆H₁₂N₂S₂Cl₂)·2H₂O]H₂O diamagnetic complex is suitable for the octahedral geometry. The appearance of bands at 32,258 and 28,902 assigned for intra-ligand transitions and

TABLE-2
KEY IR BANDS (cm⁻¹) OF H₂L AND ITS METAL COMPLEXES

Assignments	H ₂ L	Pt(IV)	Pd(II)	UO ₂ (II)	Ni(II)	Cu(II)	Co(II)
ν(OH); H ₂ O,	–	3400	3440	3440	3431	3430	3433
ν(NH)	3292	–	3167	–	3138	3150	3199
ν(C=N)	1535	1572	–	1576	–	–	–
δ(OH); H ₂ O	–	1376	1378	1350	1350	1370	1390
δ(NH)	1587	–	1571	–	1579	1570	1577
ν ^{IV} (C=S)	759	–	730	–	730	726	725
ν(C-S)	649	625	–	620	–	–	–
ν(N-N)	1031	1010	1011	1010	1015	1010	1011
δ _t (H ₂ O); δ _w (H ₂ O)	–	820; 659	826; 651	830; 658	830; 670	834; 668	853; 652
ν _{as} (OAc); ν _s (OAc)	–	1493; 1322	–	–	–	–	–
ν _{as} (NO ₃); ν _s (NO ₃)	–	–	–	1537,1399	1525; 1456	–	–
ν(M-N); ν(M-S)	–	579, 500	535, 511	530,478	504, 460	520, 480	534, 480

TABLE-3
MAGNETIC MOMENTS (BM) AND ELECTRONIC SPECTRA BANDS (cm⁻¹) OF THE LIGAND AND ITS METAL COMPLEXES

Compound	μ_{eff} (BM)	<i>d-d</i> transition (cm ⁻¹)	Intra ligand and charge transfer (cm ⁻¹)
C ₁₆ H ₁₄ N ₂ S ₂ Cl ₂ (H ₂ L)	-	-	31,847; 26,738; 23,474
[Pt ₂ (OAc) ₆ (C ₁₆ H ₁₂ N ₂ S ₂ Cl ₂)·2H ₂ O]H ₂ O	dia	-	32,258; 28,902; 25,906; 15,198
[Pd ₂ Cl ₄ (C ₁₆ H ₁₄ N ₂ S ₂ Cl ₂)]H ₂ O	dia	25,252; 23,697	32,258; 27,933
[(UO ₂) ₂ (NO ₃) ₂ (C ₁₆ H ₁₂ N ₂ S ₂ Cl ₂)·2H ₂ O]H ₂ O	dia	26,042; 23,256	40,000; 32,461, 30,000
[Ni ₂ (NO ₃) ₄ (C ₁₆ H ₁₄ N ₂ S ₂ Cl ₂)]2H ₂ O	2.9	24,697; 15,667	32,258; 28,248
[Cu ₂ Cl ₄ (C ₁₆ H ₁₄ N ₂ S ₂ Cl ₂)]2H ₂ O	1.5	23,474; 20,747	32,051; 27,933
[Co ₂ Cl ₄ (C ₁₆ H ₁₄ N ₂ S ₂ Cl ₂)]2H ₂ O	4.6	18,182; 14,881	32,258; 28,089

the bands at 25,906 and 15,198 cm⁻¹ assigned for charge transfer of S→Pt and N→Pt²⁰.

The electronic spectrum of [Pd₂Cl₄(C₁₆H₁₄N₂S₂Cl₂)]H₂O complex exhibits three spin allowed transitions from lower lying *d*-levels to the empty *d*_{x²-y² orbital. Although other two electronic transitions are also observed but their intensities are very weak and are neglected. The complex shows the absorption bands at 23,697 and 25,252 corresponding to ¹A_{1g}→¹A_{2g} and ¹A_{1g}→¹B_{1g} *d-d* transition²¹. These bands suggest that the complex possess symmetry and square planar geometry and verified through the diamagnetic appearance. Also, bands at 32,258 and 27,933 cm⁻¹ are assigned to π→π* and n→π* transition inside phenyl rings (L→MCT) (Fig. 3A).}

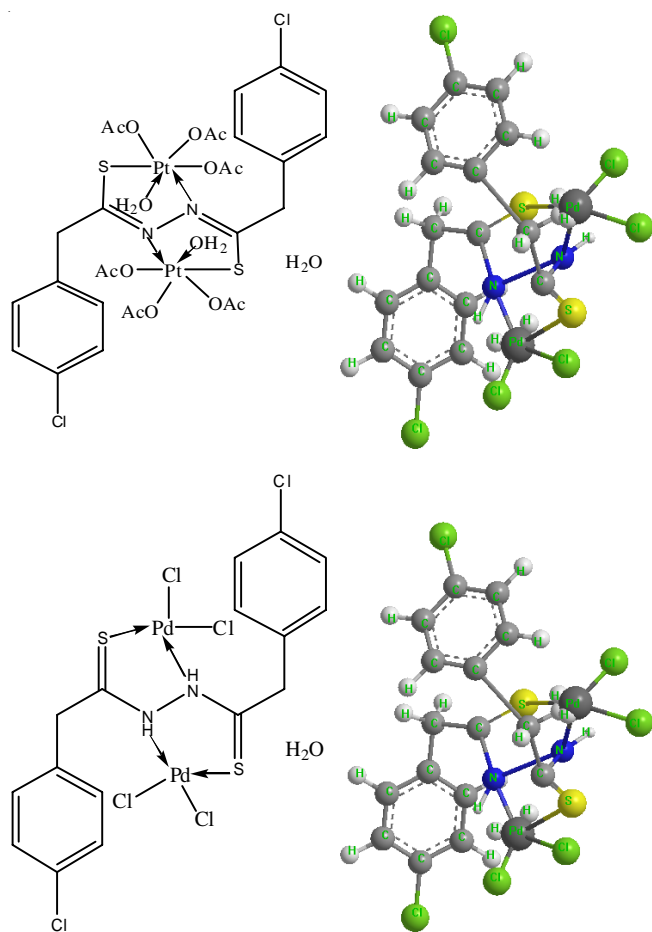


Fig. 3A. Molecular modeling and the structural formula of Pt(IV) and Pd(II) complexes

The electronic spectrum of [(UO₂)₂(NO₃)₂(C₁₆H₁₂N₂S₂Cl₂)·2H₂O]H₂O, exhibits several bands in the range of 40,000-

23,256 cm⁻¹. The bands in the region 32,461-30,000 cm⁻¹ coincide with the bands observed in the free ligand. Some of these bands are slightly shifted in comparing with the free ligand transitions because of the coordination with U(VI) ion. Two relatively less intense bands occur at 26,042 and 23,256 cm⁻¹. These can be assigned to charge transfer transition of uranyl nitrogen and sulphur, respectively²². The coordination sphere of uranium can be described as a distorted pentagonal bipyramid with the two oxygen in the apical positions with a planar equatorial coordination environment containing a molecule of bidentate NS-ligand as well as other secondary ligand molecules to complete the coordination no. (Fig. 3B). Main distortion is due to the restricting bite angles of the ligand. The spectra of [Ni₂(NO₃)₄(C₁₆H₁₄N₂S₂Cl₂)]2H₂O complex is adaptable with the octahedral geometry. The appearance of bands at 15,667 and 24,697 cm⁻¹, assigned for ³A_{2g}→³T_{1g}(F) (ν₂) and ³A_{2g}→³T_{1g}(P) (ν₃) transitions, respectively²³ proposes the octahedral configurations. The spectral ligand field parameters (10 Dq = 10,094 cm⁻¹, B = 672.94 cm⁻¹ and β = 0.646) were determined. These values are in a good agreement with those reported for six coordination *d*⁸ systems especially with SN donors²³. The magnetic moment value (2.90 BM), gives more confirmation for the suggestion (Fig. 3B).

The spectrum of [Co₂Cl₄(C₁₆H₁₄N₂S₂Cl₂)]2H₂O complex reflects the tetrahedral geometry around the Co(II) (Fig. 3C). The bands appeared at 14,881 and 18,182 cm⁻¹ could be assigned for ⁴A₂→⁴T₁ (ν₃) and LMCT transitions in a tetrahedral configuration²⁴. The magnetic moment value (4.6 BM), gives an extra evidence for this proposal. The spectral ligand field parameters (10Dq = 3774.57 cm⁻¹, B = 671.31 cm⁻¹ and β = 0.691) in which β, introduce the covalent character of the M-L bonds which is expected for the coordination with nitrogen atoms. The ligand field parameters are calculated according to the equations reported for the tetrahedral Co(II) complexes; μ_{eff} = 3.87 (1-4I/10 Dq), λ = -178 cm⁻¹

$B = [4(\nu_3 - 15Dq)^2 - 10Dq^2] / [60(\nu_3 - 15Dq) - 18Dq]$, $\nu_1 = 10Dq$.

The spectrum of [Cu₂Cl₄(C₁₆H₁₄N₂S₂Cl₂)]2H₂O complex reveals *d-d* transition band at 20,747 cm⁻¹ for ²B_{1g} → ²E_g²⁵ transition in a square-planar geometry by 1.50 BM for the *d*⁹ system and LMCT band at 23,474 cm⁻¹. Previous studies on Cu(II) complexes²⁵ (Fig. 3C) reported that the 21,785–24,750 cm⁻¹ band was due to S→Cu(II) transition nearby with the value of studied complex.

ESR spectrum: The spin Hamiltonian parameters and molecular orbital parameters of solid state Cu(II) complex are calculated (Table-4). ESR spectrum (Fig. 4) displays axially symmetric g tensor parameters with g₁₁ > g_⊥ > 2.0023

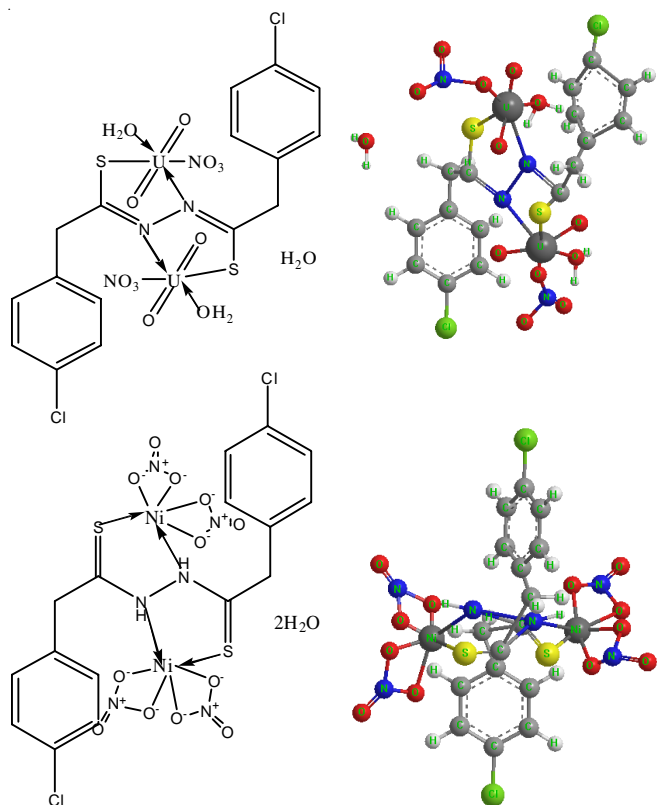


Fig. 3B. Molecular modeling and the structural formula of UO₂(II) and Ni(II) complexes

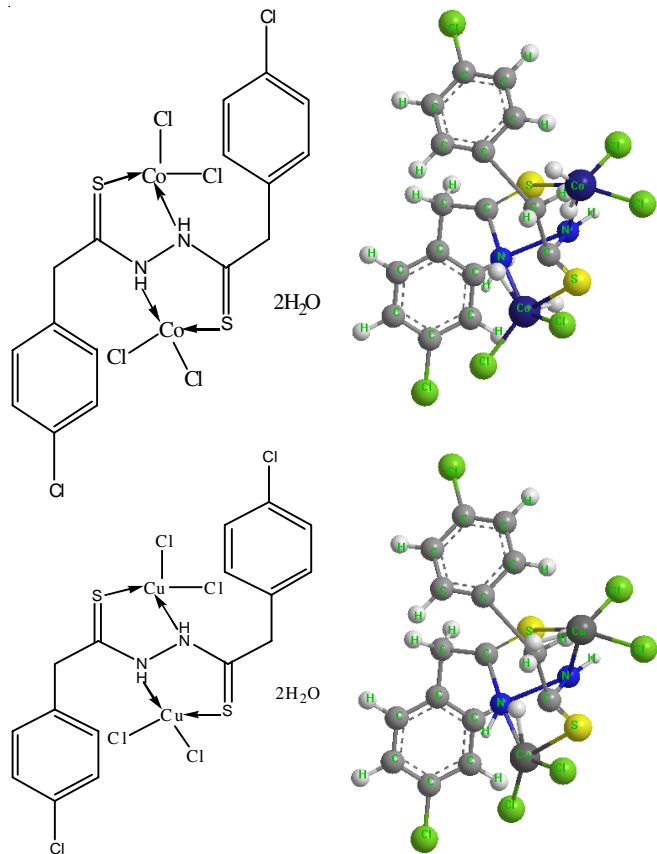


Fig. 3C. Molecular modeling and the structural formula of Co(II) and Cu(II) complexes

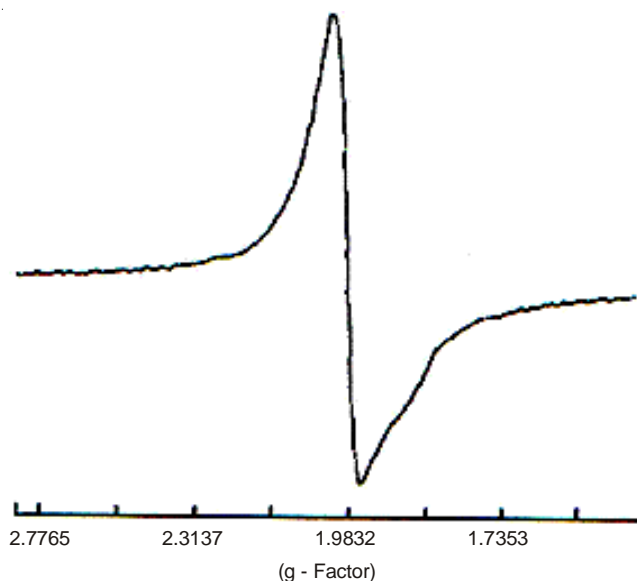


Fig. 4. ESR spectrum of solid Cu(II) complex

indicating that the $d_{x^2-y^2}$ orbital as a ground state²⁶. In axial symmetry the g -values are related to the G -factor by the expression, $G = (g_{\parallel} - 2) / (g_{\perp} - 2) = 4$, which measures the exchange interaction between copper centers in the solid. According to Hathaway and Billing²⁷, if the value of G is greater than 4, the exchange interaction between copper(II) centers in the solid state is negligible, whereas when it is less than 4, a considerable exchange interaction exists in the solid complex. The G value is less than 4 (2.86), this supports the presence of exchange coupling between copper(II) centers in the solid state²⁸. This hyperfine interaction observed for the complex is attributed to the interaction with nitrogen and oxygen nuclei adjacent to copper ion. Kivelson and Neiman²⁹ have reported the g_{\parallel} value < 2.3 for covalent character of the metal-ligand bond and > 2.3 for ionic character. Applying this criterion the covalent character of the metal-ligand bond in the complex under study can be predicated. The trigonal bipyramidal and square-pyramidal have a ground state configuration 2B_1 (unpaired electron in $d_{x^2-y^2}$ orbital) and 2A_1 (unpaired electron in d_{z^2} orbital), respectively. The tendency of A_{11} (168×10^{-4}) to decrease with increasing g_{\parallel} is an index for the increase of the tetrahedral distortion³⁰ in the coordination sphere of Cu. In order to quantify the degree of distortion of the Cu(II) complex, the f factor, $g_{\parallel}/A_{\parallel}$, (an empirical index of tetrahedral distortion)³¹ was selected from the ESR spectrum. Although its value ranges between 105 and 135 for square planar complexes, the values can be much larger in the presence of a tetrahedral distorted structure. For the investigated complex, the $g_{\parallel}/A_{\parallel}$ quotient is 125.6 cm^{-1} supporting the presence of significant dihedral angle distortion in the xy -plane and indicating a tetrahedral distortion from square-planar geometry. Molecular orbital coefficients, α^2 (A measure of the covalence of the in-plane σ -bonding between a copper $3d$ orbital and the ligand orbital) and β^2 (covalent in-plane π -bonding), were calculated by using the following equations³²⁻³⁵, where $\alpha^2 = 1$ indicates complete ionic character, whereas $\alpha^2 = 0.5$ denotes 100 % covalent bonding, with the assumption of negligibly small values of the overlap integral.

TABLE-4
ESR DATA OF Cu(II) COMPLEX AT ROOM TEMPERATURE

Complex	g_{\parallel}	g_{\perp}	g_{av}	$A_{\parallel} \times 10^{-4}$ (cm ⁻¹)	G	α^2	β^2	F
[Cu ₂ Cl ₄ (C ₁₆ H ₁₄ N ₂ S ₂ Cl ₂)]2H ₂ O	2.11	2.04	2.063	168	2.86	0.63	0.54	125.6

$$\alpha^2 = (A_{\parallel}/0.036) + (g_{\parallel} - 2.0023) + 3/7(g_{\perp} - 2.0023) + 0.04$$

$$\beta^2 = (g_{\parallel} - 2.0023) E / -8\lambda\alpha^2,$$

where $\lambda = -828 \text{ cm}^{-1}$ for the free copper ion and E is the electronic transition energy (20,747 cm⁻¹). From Table-4, the α^2 and β^2 values indicate that the in-plane σ -bonding and the in-plane π -bonding are highly covalent. The lower value of β^2 compared to α^2 indicates that the in-plane π -bonding is more covalent than the in-plane σ -bonding.

Thermo-gravimetric analysis: The TG and DTG curves were performed for the ligand and its metal complexes to describe the thermal stability of all prepared compounds. The TG curve of the ligand shows three degradation stages from 40 to 640 °C temperature region include the stepwise degradation for the organic compound ended by carbon residue. The plausible decomposition behaviour was interpreted to the data represented in Table-5. The data reveal the lower thermal stability for all investigated complexes. The degradation process was started at lower temperature ($\leq 100 \text{ }^{\circ}\text{C}$) which could be attributed to the presence of crystal water which proposed previously. The metal atoms are proposed and the residue of decomposition process which sometimes polluted with carbon atoms. The TG curves of Pt(IV), UO₂(II) and Ni(II) complexes have three degradation stages starting around 50 °C. The degradation process is introduced with a wide stage includes the removal

of water molecules, the conjugated anions and a part from the ligand. The successive degradation stages were expanded till 620-650 °C range and ended by the residual occluded metal atoms. The TG curves of Pd(II), Co(II) and Cu(II) complexes have three degradation stages except the Co(II) complex which has only two steps. The degradation process is starting around 100 °C by the removal of water molecules, the conjugated anions and a part from the ligand. The successive degradation stages were expanded till 640-660 °C range and ended by the residual occluded metal atoms polluted with carbons. The other factor may be affecting on the thermal behaviour of the complexes is the ionic radii of the central metal atoms. Somewhat observing that the greater the ionic radius of the central ion the lower the thermal stability. Such relation was relatively observed in present study as follow: Pd(II) complex (ionic radius = 0.90 Å) displays the degradation of most M-L bonds at relatively lower temperature (362 °C). The Co(II) complex (ionic radius = 0.885 Å) in which the degradation of the most metal-L bonds at 389 °C; also, Pt(IV) complex (ionic radius = 0.765 Å) displays the decomposition of most metal-L bonds at 560 °C. The UO₂(II) complex (ionic radius = 0.87 Å) the behaviour of the decomposition is not obviously attached with the ionic radius may be due to the presence of equatorial O=U=O bonds which stabilizing the complex.

TABLE-5
THERMOGRAVIMETRIC ANALYSIS DATA OF ALL INVESTIGATED COMPOUNDS

Compound	Steps	Temperature range (°C)	Decomposed assignments	Weight loss (%): Calcd. (Found)
C ₁₆ H ₁₄ N ₂ S ₂ Cl ₂ (H ₂ L)	1 st	40-240	- C ₇ H ₆ Cl	34.01 (34.11)
	2 nd	240-438	- CH ₂ N ₂ S	20.06 (20.06)
	3 rd	438-640	- C ₂ H ₆ SCI	26.42 (26.31)
	Residue		6C	19.51 (19.52)
[Pt ₂ (OAc) ₆ (C ₁₆ H ₁₂ N ₂ S ₂ Cl ₂)·2H ₂ O]H ₂ O	1 st	50-400	- 3H ₂ O + 4(OAc) + C ₈ H ₅ ClS	49.49 (49.48)
	2 nd	400-560	- C ₂ H ₃ N ₂ S	7.47 (7.47)
	3 rd	560-652	- C ₆ H ₄ Cl	9.57 (9.42)
	Residue		2Pt	33.47 (33.63)
[Pd ₂ Cl ₄ (C ₁₆ H ₁₄ N ₂ S ₂ Cl ₂)]H ₂ O	1 st	100-200	- H ₂ O + 2Cl ₂	21.54 (21.55)
	2 nd	200-362	- C ₉ H ₈ N ₂ S ₂ Cl	32.85 (32.24)
	3 rd	362-660	- C ₃ H ₆ Cl	10.45 (10.45)
	Residue		2Pd + 4C	35.16 (35.76)
[(UO ₂) ₂ (NO ₃) ₂ (C ₁₆ H ₁₂ N ₂ S ₂ Cl ₂)·2H ₂ O]H ₂ O	1 st	60-200	- 3H ₂ O + 2(NO ₃) + C ₇ H ₅ Cl	27.88 (27.87)
	2 nd	200-460	- C ₃ H ₃ N ₂ S ₂	12.09 (12.05)
	3 rd	460-625	- C ₆ H ₄ Cl	10.27 (10.26)
	Residue		(U ₂ O ₄)	49.75 (49.82)
[Ni ₂ (NO ₃) ₄ (C ₁₆ H ₁₄ N ₂ S ₂ Cl ₂)]2H ₂ O	1 st	50-240	- 2H ₂ O + 4(NO ₃) + C ₈ H ₆ SCI	58.86 (58.88)
	2 nd	240-432	- C ₂ H ₄ N ₂ S	11.43 (11.42)
	3 rd	432-622	- C ₆ H ₄ Cl	14.47 (14.46)
	Residue		2Ni	15.23(15.24)
[Co ₂ Cl ₄ (C ₁₆ H ₁₄ N ₂ S ₂ Cl ₂)]2H ₂ O	1 st	100-389	- 2H ₂ O + 2Cl ₂ + C ₈ H ₈ N ₂ SCI	56.77 (56.76)
	2 nd	389-644	- C ₆ H ₆ SCI	21.89 (21.89)
	Residue		2Co + 2C	21.33 (21.35)
[Cu ₂ Cl ₄ (C ₁₆ H ₁₄ N ₂ S ₂ Cl ₂)]2H ₂ O	1 st	90-230	- 2H ₂ O + 2Cl ₂ + C ₇ H ₆ Cl	44.99 (44.98)
	2 nd	279-320	- C ₃ H ₄ N ₂ S ₂	19.61 (19.62)
	3 rd	459-646	- C ₄ H ₄ Cl	12.98 (12.97)
	Residue		2Cu + 2C	22.41 (22.43)

X-ray diffraction studies: The X-ray powder diffraction is a very useful technique, which can introduce important structural information about the material under investigation or microcrystalline samples³⁶. The diffraction patterns were performed in the range of $5^\circ < 2\theta < 90^\circ$ for the ligand and metal-ligand complexes. Comparing the X-ray diffraction patterns of the ligand and its corresponding metal complexes indicate that the inter-planar spacing, d (Å) and the relative intensities (I/I^0) are different which could be attributed to the complex formation. The XRD patterns indicate crystalline nature for Pd(II), UO₂(II) and Ni(II) complexes as well as their original ligand. Whereas, the Pt(IV), Co(II) and Cu(II) complexes are relatively amorphous^{37,38}. This finding could be attributed to the formation of a well-defined distorted crystalline structure. Probably, this behaviour is due to the incorporation of the water molecules. A comparative study in the patterns reflects the absence of contamination of isolated complexes with starting materials. This finding was confirmed by known methods³⁹. A shift in defiant diffraction peaks of complexes was observed, suggesting the contribution of referring groups. The θ , d values (the volume average of the crystal dimension normal to diffracting plane), full width at half maximum (FWHM) of prominent intensity peak, relative intensity (%) and particle size of clearly splatting peaks were presented in Table-6. The diffraction peaks of ligand, Pd(II), UO₂(II) and Ni(II) complexes were observed at $2\theta/d$ -value (Å) = 27.11/3.29, 7.67/11.52, 9.22/7.46, 22.86/

3.89, respectively. The crystallite size was calculated from XRD patterns by applying FWHM of the characteristic peaks using Deby-Scherrer equation:

$$B = 0.94 \lambda / (S \cos \theta)$$

where S is the crystallite size, θ is the diffraction angle, B is the line width at half maximum height, $Cu/K\alpha$ (λ) = 1.5406 Å and the d -spacing were determined by using Bragg equation: $n\lambda = 2d\sin(\theta)$ at $n = 1$.

Scanning electron microscopy: Scanning electron microscopy (SEM) is a further sensitive tool used to obtain direct information about the microstructure, surface morphology and surface distribution of metal ions, surface homogeneity, particle size and chemical composition of respective compounds. The SEM images of the ligand and its Pt(IV), Pd(II), UO₂(II), Ni(II) and Cu(II) complexes were presented in Fig. 5. The images show uniform and homogeneous surface and defined metal distribution on the surface of the complex. Also, it refers to the uniformity and similarity between particle forms which indicating the existence of morphological phases and homogeneous matrix. It is evident from the SEM study that in all the synthesized metal complexes, crystals were found to grow up from just a single molecule to several molecules in an aggregate distribution with particle sizes starting from a few nanometers to several hundred. In addition, different characteristic shapes of metal complexes were identified with a quite

TABLE-6
XRD SPECTRAL DATA OF THE HIGHEST VALUE OF INTENSITY OF THE H₂L LIGAND AND ITS METAL COMPLEX

Compound	Size of particles (nm)	2θ	Intensity	d spacing (Å)	FWHM
H ₂ L	63.77	27.11	1037	3.287	0.3226
Pd ²⁺ -H ₂ L	41.61	7.67	253	11.517	0.3488
UO ₂ ²⁺ -L	9.22	11.85	124.5	7.462	1.5789
Ni ²⁺ -H ₂ L	25.86	22.86	342.9	3.887	05714

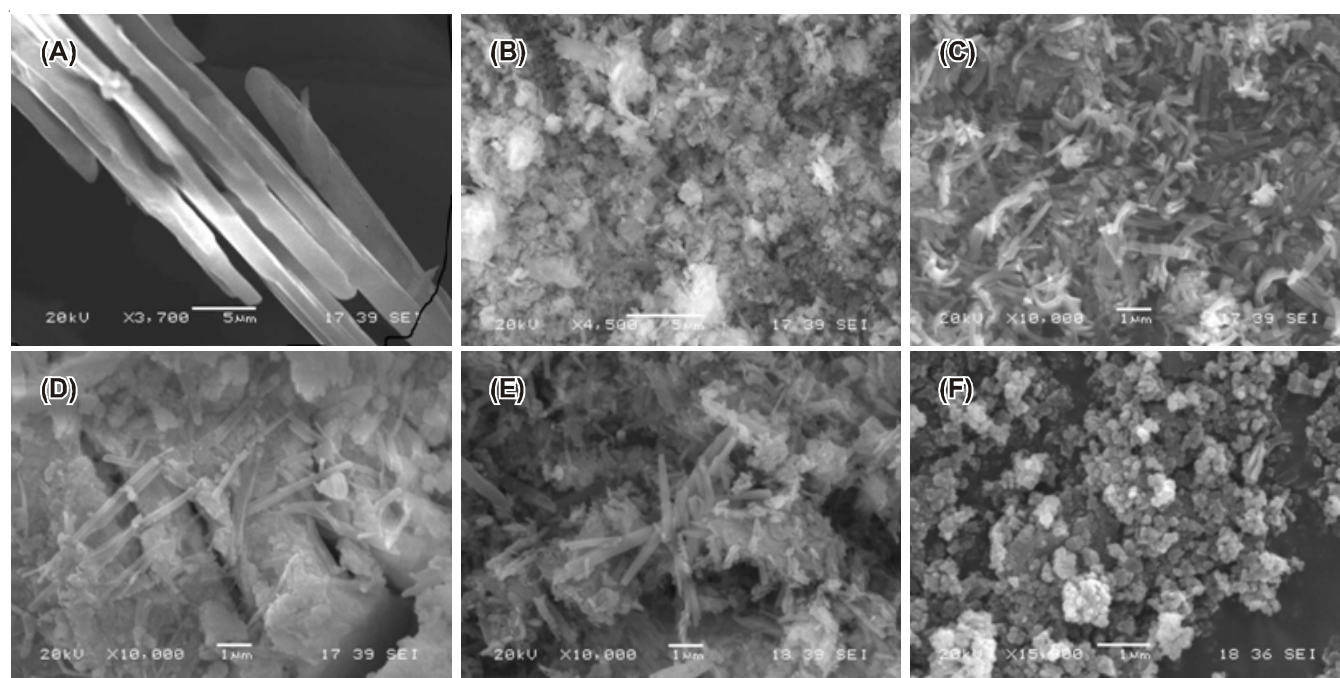


Fig. 5. Scanning electron micrographs of ligand, Pt(IV), Pd(II), UO₂(II), Ni(II) and Cu(II) (A, B, C, D, E and F, respectively) inset shows the magnified image

difference from that of the free ligand. The difference in the shape of the metal complexes crystal aggregates deposited on the thin films was mainly dependent on the metal ions. On the other hand, it can be seen a rock like appearance with a numerous territorial patches were observed with all scanned samples except the free ligand and the Cu(II) complex. These may suggest the amorphous nature of the investigated complexes except the Cu(II) one with complicated interpretation due to unclear appearance. Estimated size ranges are found to be: 0.1-0.2 μm for the Cu(II) complex. A significant difference in-between the XRD and SEM investigation tools are the main cause for the unmatched results, but the most preferable one is considered XRD technique.

Computational study: A trials were carried out to gain a better insight on the most suitable geometry of the ligand to propose the bonding mode. Here, we calculate some theoretical parameters and the results are in accordance with the experimental data. Molecular total energy of the ligand in two form as follow: -3.1631 and -0.5218 Kcal/mol for thione-thiol (Fig. 1), respectively. This suggesting the relative high stability of thione form in comparing with another tautomer, such verify the tendency of its coordination observed. Finally, the optimized structure of the thione form is clearly angular bended where the phenyl rings almost parallel to each other which is too close to the x-ray structure of analogue compound^{40,41}. To shed light, metal complexes were optimized using semi-empirical PM3 method. As shown in Fig. 3, the lowest internal energy of the molecular structures as follow: 716.606, 35.2704, -32.8775, 240.6123, -12.8661 and -12.7538 Pt(IV), Pd(II), UO₂(II), Ni(II), Cu(II) and Co(II). The calculated internal energy represents the stability of UO₂(II), Cu(II) and Co(II) complexes. The optimized structures of Co(II) is tetrahedral as well as the Ni(II), Pt(IV) and UO₂(II) are octahedral. While, Pd(II) and Cu(II) are square planar structures. Also implementing the program reveals lengthen in the bonds of the function groups concerned in complexation from (2)C=S(4) = 1.313 and (3)N-N(5) = 1.113 values in the original ligand. This indicating the participation of high electron dense atoms (SNNS) in coordination.

REFERENCES

- M. Keeton, *Coord. Chem. Rev.*, **13**, 279 (1974).
- S.N. Pandeya and J.R. Dimmock, *Pharmazie*, **48**, 659 (1993).
- M.A. Ali and S.E. Livingiston, *Coord. Chem. Rev.*, **13**, 101 (1974).
- D.W. West, S.B. Padhye and P.B. Sonawane, *Struct. Bonding*, **76**, 1 (1991).
- A.K. El-Sawaf, D.X. West, R.M. El-Bahnasawy and F.A. El-Saied, *Transition Met. Chem.*, **23**, 227 (1998).
- M. Joseph, M. Kuriakose, M.R.P. Kurup, E. Suresh, A. Kishore and S.G. Bhat, *Polyhedron*, **25**, 61 (2006).
- N.L. Allinger, *J. Am. Chem. Soc.*, **99**, 8127 (1977).
- Hyper-Chem Professional 7.5, Hypercube, Inc., Gainesville, FL 32601, USA (2002).
- A.I. Vogel, Text Book of Quantitative Inorganic Analysis, Longman, London (1986).
- W.J. Geary, *Coord. Chem. Rev.*, **7**, 81 (1971).
- M.S. Refat, *Spectrochim. Acta A*, **68**, 1393 (2007).
- N.M. El Metwally, R. Arafa and U. El-Ayaan, *J. Therm. Anal. Calorim.*, **8**, 3065 (2013).
- U. El-Ayaan, M.M. Youssef and S. Al-Shihry, *J. Mol. Struct.*, **936**, 213 (2009).
- K.S. Siddiqi, R.I. Kureshy, N.H. Khan, S. Tabassum and S.A.A. Zaidi, *Inorg. Chim. Acta*, **151**, 95 (1988).
- G.A.A. Al-Hazmi, A.A. El-Zahhar, K.S. Abou-Melha, F.A. Saad, M.H. Abdel-Rhman, A.M. Khedr and N.M. El-Metwaly, *J. Coord. Chem.*, **68**, 993 (2015).
- S.J. Swamy and K. Bhaskar, *Indian J. Chem.*, **38A**, 961 (1999).
- ZakiMohamed, Z.M. Zaki and G.G. Mohamed, *Spectrochim. Acta A*, **56**, 1245 (2000).
- McGlynn and Smith. S.P. McGlynn and J.K. Smith, *J. Mol. Spectrosc.*, **6**, 188 (1961).
- A.A. El-Asmy, M.E. Khalifa and M.M. Hassanian, *Synth. React. Inorg. Met. Org. Chem.*, **31**, 1787 (2001).
- R. Srinivasan, I. Sougandi, R. Venkatesan and P.S. Rao, *Proc. Indian Acad. Sci. Chem.*, **115**, 91 (2003).
- A.B.P. Lever, Inorganic Electronic Spectroscopy, Elsevier, Amsterdam, edn 2 (1984).
- D.-R. Zhu, Y. Song, Y. Xu, Y. Zhang, S.S. Sundara Raj, H.-K. Fun and X.-Z. You, *Polyhedron*, **19**, 2019 (2000).
- S. Chandrasekhar and A. McAuley, *Inorg. Chem.*, **31**, 2234 (1992).
- A.A. El-Asmy, A.Z. El-Sonbati, A.A. Ba-Issa and M. Mounir, *Transition Met. Chem.*, **15**, 222 (1990).
- M.S. Refat and N.M. El-Metwaly, *Spectrochim. Acta A*, **92**, 336 (2012).
- H.I. Park and L.J. Ming, *J. Inorg. Biochem.*, **72**, 57 (1998).
- (a) B.J. Hathaway and D.E. Billing, *Coord. Chem. Rev.*, **5**, 143 (1970); (b) B.J. Hathaway, *Struct. Bonding*, **57**, 55 (1984).
- H. Montgomery and E.C. Lingafelter, *Acta Crystallogr.*, **20**, 728 (1966).
- D. Kivelson and R. Neiman, *J. Chem. Phys.*, **35**, 149 (1961).
- J.A. Welleman, F.B. Hulsbergen, J. Verbiest and J. Reedijk, *J. Inorg. Nucl. Chem.*, **40**, 143 (1978).
- H. Yokoi and A.W. Addison, *Inorg. Chem.*, **16**, 1341 (1977).
- R.K. Ray and G.B. Kauffman, *Inorg. Chim. Acta*, **174**, 257 (1990).
- K. Jayasubramanian, S.A. Samath, S. Thambidurai, R. Murugesan and S.K. Ramalingam, *Transition Met. Chem.*, **20**, 76 (1995).
- V.S.X. Anthonisamy and R. Murugesan, *Chem. Phys. Lett.*, **287**, 353 (1998).
- V.S.X. Anthonisamy, R. Anantharam and R. Murugesan, *Spectrochim. Acta A*, **55**, 135 (1999).
- A.A. Fahem, *Spectrochim. Acta A*, **88**, 10 (2012).
- A. Shahrjerdi, S.S.H. Davarani, E. Najafi and M.M. Amini, *Ultrason. Sonochem.*, **22**, 382 (2015).
- B.D. Cullity, Elements of X-ray Diffraction, Addison-Wesley Inc., edn 3 (1993).
- B.D. Cullity, Elements of X-ray Diffraction, Addison-Wesley Mass, edn 2 (1978).
- M.H. Abdel-Rhman, M.M. Hassanian and A.A. El-Asmy, *J. Mol. Struct.*, **1019**, 110 (2012).
- H. Beraldo, W.F. Nacif and D.X. West, *Spectrochim. Acta A*, **57**, 1847 (2001).